ROLE OF DIELECTRIC CONSTANT IN ELECTROHYDRODYNAMICS OF CONDUCTING FLUIDS

Percy H. Rhodes

National Aeronautics and Space Administration

George C. Marshall Space Flight Center

Code ES76, Huntsville, Alabama 35812

Robert S. Snyder

National Aeronautics and Space Administration

George C. Marshall Space Flight Center

Code ES73, Huntsville, Alabama 35812

Glyn O. Roberts

Roberts Associates Incorporated

11794 Great Owl Circle

Reston, Virginia 22094

ROLE OF DIELECTRIC CONSTANT IN CONDUCTING FLUIDS

Percy H. Rhodes

Code ES76

Marshall Space Flight Center, AL 35812

ABSTRACT

Electrohydrodynamic (EHD) flows are driven by the interaction of an electric field with variations in electric conductivity or dielectric constant. In reported EHD experiments on the deformation of drops of immiscible dielectric fluids, the role of conductivity has tended to overshadow the role of dielectric constant. Often, large conductivity contrasts were convenient because the conductivities of the dielectric fluid were relatively uncertain. As a result, the observed effects were always qualitatively the same as if there had been no contrast in dielectric constant.

Our early experiments (5) studying the EHD deformations of cylindrical streams readily showed the conductivity effect but the dielectric constant effect was not discernible. We have modified our flow chamber and improved our method of observation and can now see an unequivocal dielectric constant effect which is in agreement with the theory given in (5).

In this paper we first give a brief description of the physics of charge buildup at the interface of an immersed spherical drop or flowing cylindrical sample stream and then show how these charge distributions lead to interface distortions and accompanying viscous flows which constitute EHD. We next review theory and experiment describing the deformation of spherical drops. We show that in the reported drop deformation experiments, the contrast in dielectric constant was never sufficient to reverse the deformation due to the conductivity contrast.

We review our work (5) describing the deformation of a cylindrical stream of one fluid flowing in a parallel flow of another, and we compare the deformation equations with those for spherical drops. Finally, we show a definite experimental dielectric constant effect for a cylindrical stream of aqueous polystyrene latex suspension. The dielectric constant varies with the frequency of the imposed electric field, and the associated EHD flow change is very apparent.

Introduction

Electrohydrodynamics (EHD) describes fluid flows driven by external electric fields and by the charge and polarization distributions induced by those fields. These flows are thus generally proportional to the square of the imposed electric field. For alternating current (AC), the steady component of the flow is proportional to the mean square field. The oscillatory component of the flow (with doubled frequency) is generally negligible, because momentum keeps it small, or because it oscillates and gets nowhere.

By way of contrast, consider the common occurrence of electroosmotic flow in an open fluid system as shown in Figure 1. The wall carries a net negative charge and hence attracts positive counter-ions from the fluid to form a positive charge layer (double layer) at the wall. The presence of the electric field causes these hydrated positive ions to move toward the negative electrode. The viscous action of the fluid extends this motion throughout the chamber to cause a plug flow to the right, toward the negative electrode. Note that the charge distribution is present even when there is no imposed electric field, and that the flow is therefore proportional to the imposed field. With AC, there is no steady component to the electroosmosis flow, and the oscillation is generally of no importance.

Induced Charge and Transients Time Scale in EHD

We now analyze how external fields establish a charge distribution. From charge continuity, Ohm's law, and Maxwell's equations,

$$\begin{aligned} \dot{q}_v &= -\nabla \cdot \vec{j} \\ &= -\nabla \cdot (\sigma \vec{D} / K) \\ &= -\vec{D} \cdot \nabla(\sigma / K) - (4\pi\sigma / K) q_v . \end{aligned} \qquad [1]$$

Here q_v is the volume charge density, and σ and K are the conductivity and dielectric constant. We are using electrostatic units (esu), so that K is also the electrical permittivity. The vectors $\vec{j}$ and $\vec{D}$ are the current density and electric displacement, given in terms of the electric field by

$$\vec{j} = \sigma\vec{E},$$
$$\vec{D} = K\vec{E}.$$

Equation [1] shows first that transient charges decay in a time ($K/4\pi\sigma$), which is of order 10^{-9} seconds or less for practical aqueous fluids. Secondly, the charge density approaches the value given by setting the left hand side of Eq. [1] to zero. The quasi-steady volume charge density is

$$\begin{aligned} 4\pi q_v &= -(K/\sigma)\vec{D}\cdot\nabla(\sigma/K) \\ &= +(\sigma/K)\vec{D}\cdot\nabla(K/\sigma) \\ &= +\vec{j}\cdot\nabla(K/\sigma). \end{aligned} \qquad [2]$$

The post-transient quasi-steady charge density q_v is non zero whenever the ratio K/σ varies along the field lines. And third, after the charge distribution has been established,

$$\nabla\cdot\vec{j} = 0. \qquad [3]$$

This equation is solved for the potential distribution in any particular case.

The analogous equation for the transient surface charge density q_s at an interface is

$$\dot{q}_s = -j_{n2} + j_{n1}. \qquad [4]$$

The normal component j_n of the current density is measured from side 1 to side 2 of the interface, and the difference of the two values determines the rate of increase of the surface charge density q_s. Using

$$\vec{j} = (\sigma / K)\vec{D}, \qquad [5]$$

and a difference identity,

$$\begin{aligned} \dot{q}_s &= -\overline{D_n}(\sigma_2 / K_2 - \sigma_1 / K_1) - (\overline{\sigma / K})(D_{n2} - D_{n1}) \\ &= -\overline{D_n}(\sigma_2 / K_2 - \sigma_1 / K_1) - (\overline{\sigma / K})(4\pi q_s). \end{aligned} \qquad [6]$$

Here the overbars denote averages of the values on the two sides of the interface. The quantity $4\pi q_s$ is the jump in the normal component of $\vec{D}$. The q_s multiplier is the reciprocal of the transient time scale, as before. Once the transients have decayed, the two normal components of $\vec{j}$ are equal in Eq. [4], and the quasi-steady surface charge is given by

$$\begin{aligned} 4\pi q_s &= D_{n2} - D_{n1} \\ &= j_n(K_2 / \sigma_2 - K_1 / \sigma_1). \end{aligned} \qquad [7]$$

This equation is closely analogous to Eq. [2] for the continuous case.

Induced Charge for a Drop or Cylinder

In this study we consider the EHD flows associated with spheres or circular cylinders of an inside fluid in a surrounding outside fluid. We review theoretical and experimental work done by others and ourselves, and attempt to explain their structure and sign physically. Figure 2 shows

the spherical or cylindrical geometry, and adds electrodes to indicate an imposed field direction from left to right.

From Eq.s [1] and [2] there is no induced charge in the homogeneous regions. Charge is induced only at the interface.

From Eq. [7] the surface charge is

$$4\pi q_s = j_n(K_o / \sigma_o - K_i / \sigma_i). \qquad [8]$$

Defining the conductivity and dielectric constant ratios as

$$R = \sigma_i / \sigma_o, \qquad [9]$$

$$S = K_i / K_o, \qquad [10]$$

Equation [8] can be rewritten as

$$4\pi q_s = (R - S) j_n K_o / \sigma_i. \qquad [11]$$

The current in Figure 2 is from left to right. So on the right half of the interface the outward normal current j_n is positive, and the interface charge density q_s has the same sign as $(R\text{-}S)$. Thus q_s is negative on the right in Figure 2a, where

$$R < 1 < S\,. \qquad [12]$$

and positive on the right in Figure 2b, where

$$R > 1 > S . \qquad [13]$$

On the left half of the interfaces in Figure 2, the outward normal current j_n is negative, and the induced charge in Figures 2a and 2b has the opposite sign, as shown.

Flow Calculation

Once the electric field solution and the associated induced charge density have been found, the corresponding flow is determined by solving the Navier-Stokes equations, with the electric forces included. The electric forces can be equivalently expressed either in terms of the Maxwell stress tensor (convenient for interface boundary conditions) or as the sum of the electric forces on the charge density and on the dipole distribution associated with the dielectric constant.

On the scales of interest, fluid momentum can normally be neglected. The flow is therefore a balance between the electric forces, viscosity, and pressure gradients, with the incompressibility condition. Interface surface tension must be included in determining the change of shape of drops.

We have chosen not to give details in this review. But inspection of Figure 2a suggests that with the electric field from left to right, the electric forces pull the positive and negative charges towards each other, flattening the circle normal to the electric field. And in Figure 2b, the electric forces on the positive and negative surface charge distributions pull them apart, tending to elongate the circle toward the electrodes.

This is confirmed by the detailed computations for the drop and cylindrical geometries. For the two special cases (12) and (13) shown in Figures 2a and 2b, the inclusion of the dipole electric forces does not change the solution qualitatively.

On the other hand, when R and S are either both greater than unity or both less than unity, dielectric forces can change the qualitative picture. In particular, Eq. [11] shows that for $R = S$ there is no induced charge on the surface. But the detailed calculations show non zero EHD flow in this case, except in the trivial case $R = S = 1$.

Theory of Drop Deformation

This early work on EHD flows was concerned with drop deformation, and used immiscible fluids. A neutrally buoyant spherical drop of one fluid in the other distorted against surface tension by the application of a uniform AC field, and the shape distortion was measured and compared with theory.

The theory for conducting fluids was given by Taylor (1), and is known as Taylor's "leaky dielectric" model. Taylor obtains the drop deformation (defined as the difference of the drop axis lengths (diameters) divided by their sum, and positive for a prolate spheroid) in the form

$$\Omega = \frac{9}{64}\left[\frac{K_o a E^2}{\pi\gamma(2+R)^2}\right]\Phi. \qquad [14]$$

In this equation, γ is the surface tension, a the drop radius, E the imposed root mean square electric field, and the dimensionless discriminating function is

$$\Phi = 1 + R^2 - 2S + N(R - S). \qquad [15]$$

Here

$$N = \frac{6M + 9}{5M + 5}, \qquad [16]$$

$$M = \mu_i / \mu_o, \qquad [17]$$

and μ_i and μ_o are the inner and outer viscosities. Thus N decreases from 1.8 to 1.2 as the viscosity ratio M increases from zero to infinity, and is 1.5 when M is 1. Note that Taylor used the reciprocal S definition to our Eq. [10], so we have changed his results appropriately to obtain our Eqs. [14] and [15].

If Φ is positive, the spherical drop is elongated in the electric field direction, into a prolate spheroid. If Φ is negative, the drop is flattened normal to the electric field direction, into an oblate spheroid.

Drop Deformation Experiments

Many reported EHD studies have measured the electrical deformation of spherical drops, using various combinations of immiscible fluids. In this review, we emphasize the significance of dielectric constant effects. In our view, none of these reported results unequivocally demonstrated such effects, since in all cases the sign of the discriminating function (6) was the same as if the dielectric constant ratio had been 1. Note that from Eq. [6] the critical value of the dielectric constant ratio S is

$$S(R) = \frac{1 + NR + R^2}{2 + N}. \qquad [18]$$

Figure 4 shows the critical S value as a function of R ,for the three N values indicated. Note that the viscosity ratio plays only a minor role. For subcritical S values (below and to the right of the curve), the drop becomes a prolate ellipsoid, elongated in the field direction. For supercritical S values (above and to the left of the curve), the drop becomes an oblate ellipsoid, flattened normal to the field direction. Intermediate R values have been avoided in the reported results, apparently due to the conductivity difficulties. For large R, the critical S value is very large, while for R close to zero, it is just $1/(2+N)$, or about 0.3, as figure 4 shows.

An unequivocal demonstration of a dielectric constant effect in EHD requires a sign change in the drop distortion. For $R < 1$ this requires that S is less than the critical value, while for $R > 1$ it requires that S is greater than the critical value. Otherwise we can say that the sign of the discriminating function ϕ given by Eq. [15] is "controlled" by R.

In these admittedly difficult experiments, measuring and controlling the conductivities and controlling the interface surface tension are often the hardest problems. Fortunately, in Eq. [14], $\Phi/(2+R)^2$ simplifies to 1 for large conductivity ratio R and to $(1-2S-NS)/4$ for small R.

Allan and Mason (2) reported drop deformation experiments with 13 different combinations of fluids. In all cases the observed deformation correlated with Φ, and was also that expected for the measured conductivity ratio R. The experimental R values ranged up from 15, or down from 1/15. In terms of Eqs. [14] and [15], these experiments did not demonstrate a dielectric effect; the results were qualitatively the same as if S had been unity.

Concerning the difficulty of these drop experiments, Melcher and Taylor (7) make the following statement. "Electrostatic effects in fluids are known for their vagaries: often they are so extremely dependent on electrical conductivity that investigators are discouraged from carefully analytic models and simple experiments." The problems include maintaining purity and consistency for the sample fluids, and conductivity changes due to diffusion of solutes across the interface.

Torza, Cox, and Mason (3) reported 22 fluid combinations, which were all controlled by the conductivity ratio R. Similarly, Vizika and Saville (4) reported 11 fluid combinations; also controlled by R. In the small R cases in (2) through (4), the smallest S value was 0.44, or substantially above the critical value of $1/(2+N)$. A smaller value would have provided an unequivocal demonstration of dielectric constant effects in EHD.

Dielectric Constant of Aqueous Suspensions

Clays and aqueous suspensions can be polarized, and act as homogeneous fluids with very high dielectric constants. This phenomenon is associated with the electrochemical charge double layer on each particle, like the layer shown earlier in Figure 1. As the particle and its surrounding charge cloud respond to the external field, and undergo electroosmosis, they also become a dipole. The higher the frequency for AC, the less time there is for the charge to move. Thus K decreases with increasing frequency, as shown in Figure 3.

The dielectric constant of a suspension is measured experimentally by using an accurate bridge technique to determine the complex resistance of an electrolytic cell, as a function of frequency. This is not easy, and comparisons with theory have been mixed.

We are interested in supplementing existing techniques by using EHD as an independent method for determining the dielectric constant of suspensions.

Over the last several years we have studied the deformation of cylindrical sample streams consisting of dispersions of polystyrene latex (PSL) microspheres (5,6). The sample is drawn into a fine filament as it is injected into a flowing carrier buffer. The major difference between our system and the immiscible drop system discussed previously is the absence of surface tension in our case. The application of a uniform electric field to the cylindrical sample filament will progressively distort the sample stream into a ribbon. The orientation of the ribbon depends on the ratios of dielectric constant and electrical conductivity between the buffer and sample. These distortions are the result of EHD flows in both the sample and buffer. The leaky dielectric model of Taylor is again used to determine the degree and orientation of the sample stream distortion.

For a circular sample stream of properties shown in Figure 2, we showed (5) that the radial EHD velocity u at the interface is given by

$$u = FD \cos 2\theta , \qquad [19]$$

where the amplitude function is

$$F = \frac{aE^2K_o}{12\pi(\mu_i + \mu_o)(R+1)^2} \qquad [20]$$

and the discriminating function is

$$D = R^2 + R + 1 - 3S . \qquad [21]$$

Here θ is the polar coordinate angle measured from the electric field direction. Note that the angular dependence cos 2θ implies distortion of the circular sample section to an ellipse. From qualitative theoretical study (5) and from all our observations, this distortion continues until the sample becomes a flattened ribbon, either aligned with the field or perpendicular to it.

Note the similarity between this discrimination function D given by Eq. [21], and the earlier function Φ for drop deformation, given by Eq. [15]. Both are different from the approximate discriminating function (R-S) suggested by Eq. [11] and by the qualitative approximation of considering only the forces on free charges in computing the flow. Remarkably, Eq. [21] can be obtained from Eq. [15] by setting the function N of the viscosity ratio to unity. The critical S(R) for a cylinder makes D zero, and is shown in Figure 4, with the corresponding plots for drops. At smaller S values, the cylinder elongates in the field direction, forming first an ellipse and then a ribbon.

Limitations of the Theory

There are a number of problems with the theory and with its application to our experiments using nozzle injection to produce a circular cylinder with a sharp interface.

The solution is valid only as long as the sample stays approximately circular. It can't describe the late stages of collapse to a ribbon; nor can it even guarantee that all cases will eventually collapse to a ribbon. Further, if the ribbon has only been deformed a little, measurements of the deformation must be less precise. Precise determinations can still be made, for example, of conditions for the sample to remain circular.

The solution is poor close to the nozzle, since the nozzle distorts both the electric field distribution and the flow of both fluids. Equating time with distance downstream from the nozzle divided by some mean speed is not accurate. Better accuracy is possible by taking an origin perhaps 5 diameters downstream from the nozzle, and observing the further distortion from that point onward.

The assumption of an infinite fluid is wrong; there are chamber boundaries at some finite distance. So is the neglect of momentum; at some large distance momentum forces become comparable with viscous forces. Both problems are minor; the relative error involved in the flow near the cylinder is of order the square of the ratio of the cylinder radius to the larger distance.

The application of a "two-dimensions-plus-time" formulation, with downstream derivatives neglected or approximated, is approximately valid only away from the nozzle and from the chamber walls, and only if the downstream length scale is large compared with the cylinder radius.

The assumption of a discontinuity in conductivity and dielectric constant is invalid, since there will be diffusion near the interface. But solute diffusivities are very low, while particle diffusivities are zero. The flow speeds are low and the length scale small, so there is no turbulent mixing. And both analytic and numerical studies have convinced us that whether the interface change is discontinuous or is spread smoothly over even a quarter of the radius, it makes very little difference to the flow solution.

PSL Sample Stream Distortion Experiments

In our experiments with sample stream distortion, we could vary the conductivity of both fluids. But we could not at first find a dielectric constant effect. Part of the problem was the low sensitivity of our early system, which was an electrophoresis type chamber limited to 30 V/cm. In addition, we were expecting K values from 200 to 1000 and higher, based on published literature for PSL suspensions. In fact, it appears that our samples were much closer to the water and buffer K value of 80.

We improved the sensitivity of our method by using a small square chamber, allowing fields up to 300 V/cm, and by observing the distorted stream using a microscope system with a CCD camera and video monitor, at 62.5 magnification. Physically, the sample stream distortion was increased by a factor of 100, because of the E^2 dependence shown in Eq. [14]. Thus, our sensitivity improved by a factor of 6,250.

With this system we have been able to demonstrate the EHD effects of the variations of dielectric constant with frequency, as shown in Figure 3. These demonstrations are now repeatable.

Figure 5 shows eight views of steady EHD flows in our apparatus. The eight percent sample is injected through the circular nozzle just visible on the right. The transparent buffer, with matched conductivity, also enters the chamber from the right.

In Figure 5a there is no applied field, and the PSL passes along the chamber as a circular cylinder of constant diameter. The changes in cylinder diameter near the nozzle are associated with the nozzle drag on the buffer and PSL flow and with the viscous adjustment to a more uniform downstream flow profile.

In the rest of Figure 5 there is a fixed external AC electric field in the viewing direction; only the frequency is varied. No changes are made in the buffer or sample fluids or flow rates. In Figure 5b, at 100,000 Hz, R and S are 1, and there is no EHD flow. At lower frequencies S increases, according to Figure 3 and Eq. [10]. This makes the discriminant (21) increasingly negative, so that the circular sample stream is progressively flattened into a ribbon normal to the field, as it passes downstream to the left. For the lowest frequency of 28 Hz, this flattening is very rapid.

This series of photographs vividly shows the dielectric constant effect on EHD, and its variation with frequency, for a PSL sample filament. It also suggests a method for the measurement of dielectric constant. The stream at each frequency can be brought to zero deformation by adjustment of the conductivity ratio R. This value of R can then be used in Eq. [21] (with $D = 0$) to calculate S and, hence, K_i.

The PSL particles were made using a recipe without emulsifier, and each polymer (styrene) chain is terminated with a sulfate and end group at each end. The sample was sonicated and centrifuged, and then placed in phosphate buffer to form the sample stock. The final conductivity was adjusted using distilled water. The buffer used had a pH of 7.08.

Conclusions

We believe that the sample stream distortions which are shown in Figure 5 are the first experimental evidence of the dielectric constant effect in conducting fluids to appear in the literature. We are continuing work on our miniature flow chamber to improve the uniformity of the electric field while still maintaining clear observation of the sample stream when viewed parallel to the field. We will now quantify a selection of PSL with respect to debye length (κ^{-1}), zeta potential ζ, and particle radius a. The dielectric constant of this selection can then be

determined as a function of frequency ν by the method previously described. This data will then be described by a Cole-Cole relaxation frequency distribution which can be compared to the standard model of Delacy and White (8) and to dielectric spectroscopy measurements of Myers and Saville (9).

REFERENCES

1. Taylor, G. I., *Proc. R. Soc. London,* **291**, 159 (1966.

2. Allan, R. S., and Mason, S. G., *Proc. R. Soc. London,* A **267**, 45 (1962).

3. Torza, S., Cox, R. G., and Mason, S. G., *Phil. Trans. R. Soc. London,* **269**, 259 (1971).

4. Vizika, O., and Saville, D. A., *J. Fluid Mech.*, **239**, 1 (1992).

5. Rhodes, P. H., Snyder, R. S., and Roberts, G. O., *J. Colloid Interface Sci.*, **129**, 78 (1989).

6. Rhodes, P. H., Snyder, R. S., Roberts, G. O., and Baygents, J. C., *Applied and Theoretical Electrophoresis,* **2/3**, 87 (1991).

7. Melcher, J. R., and Taylor, G. I., *Ann. Rev. Fluid Mech.*, **1**, 111 (1969).

8. Delacey, E. B., and White L. R., *J. Chem. Soc. Faraday Trans.*, 2, **77**, 2007 (1981).

9. Myers, D. F., and Saville, D. A., *J. Colloid Interface Sci.*, **131**, 461 (1989).

Figure Legends

Fig. 1. Electroosmotic flow example.

Fig. 2. Charge distribution at the interface and resulting EHD flows. (a) Charge distribution for $K_1 > K_0$ and $\sigma_i < \sigma_0$ producing distortion normal to the field (oblate). (b) Charge distribution for $K_1 < K_0$ and $\sigma_i > \sigma_0$ producing distortion parallel to the field (prolate).

Fig. 3. Variation of dielectric constant with frequency v for a typical PSL suspension.

Fig. 4. Critical dielectric constant ratio as a function of the conductivity ratio, for drops and cylinders. For drops, N is the function (16) of the viscosity ratio. Below and to the right of the critical value curve, the drop or cylinder elongates in the field direction.

Fig. 5. Sample stream distortions viewed parallel to the AC electric fields at varying frequency. 8% PSL. (a) 100 volts RMS. 28 Hz frequency. (b) 100 volts RMS. 100 Hz frequency. (c) 100 volts RMS. 1000 Hz frequency. (d) 100 volts RMS. 5000 Hz frequency. (e) 100 volts RMS. 10000 Hz frequency. (f) 100 volts RMS. 50000 Hz frequency. (g) 100 volts RMS. 100000 Hz frequency. (h) Zero electric field.

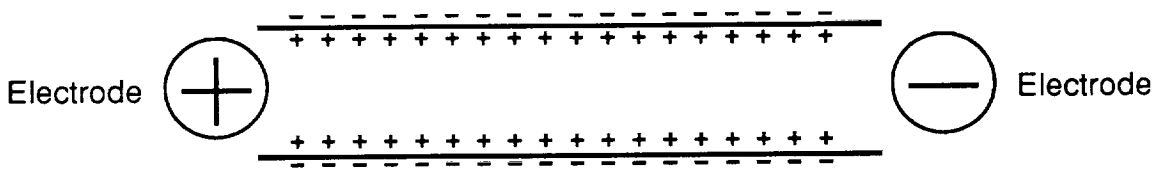

Figure 1. Electroosmotic Flow Example

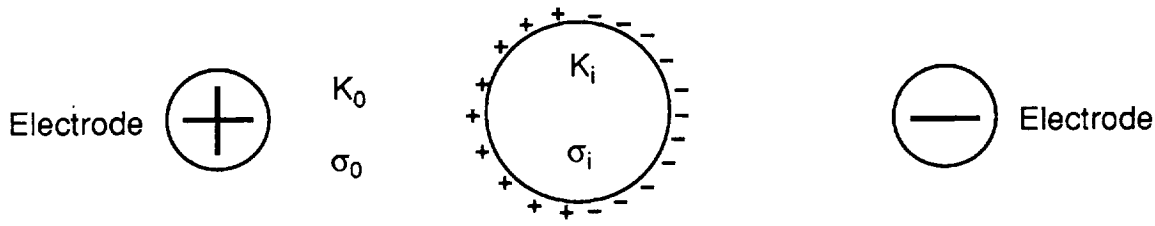

Fig. 2a. Charge distribution for $K_i > K_0$ and $\sigma_i < \sigma_0$ producing distortion normal to the field (oblate)

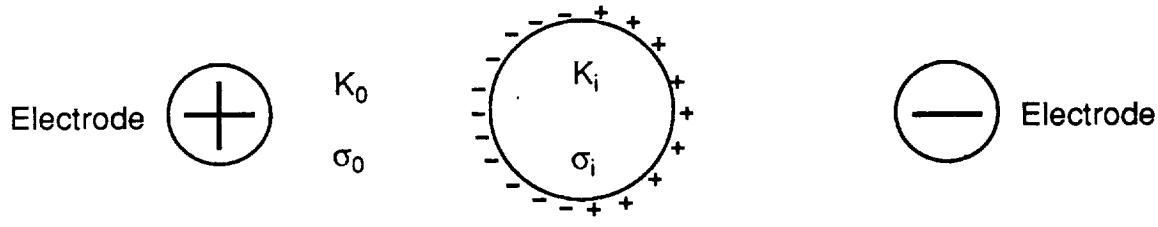

Fig. 2b. Charge distribution for $K_i < K_0$ and $\sigma_i > \sigma_0$ producing distortion parallel to the field (prolate)

Figure 2. Charge Distribution at the Interface and Resulting EHD Flows

5-21567

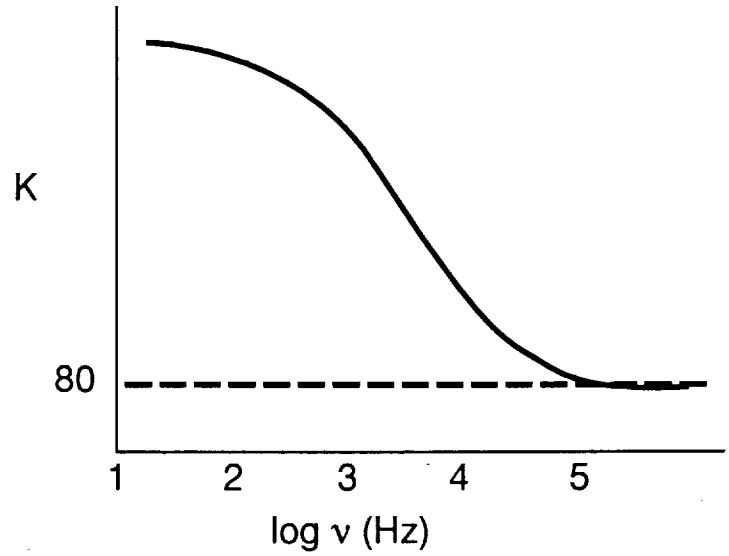

Figure 3. Variation of dielectric constant with frequency ν for a typical PSL suspension

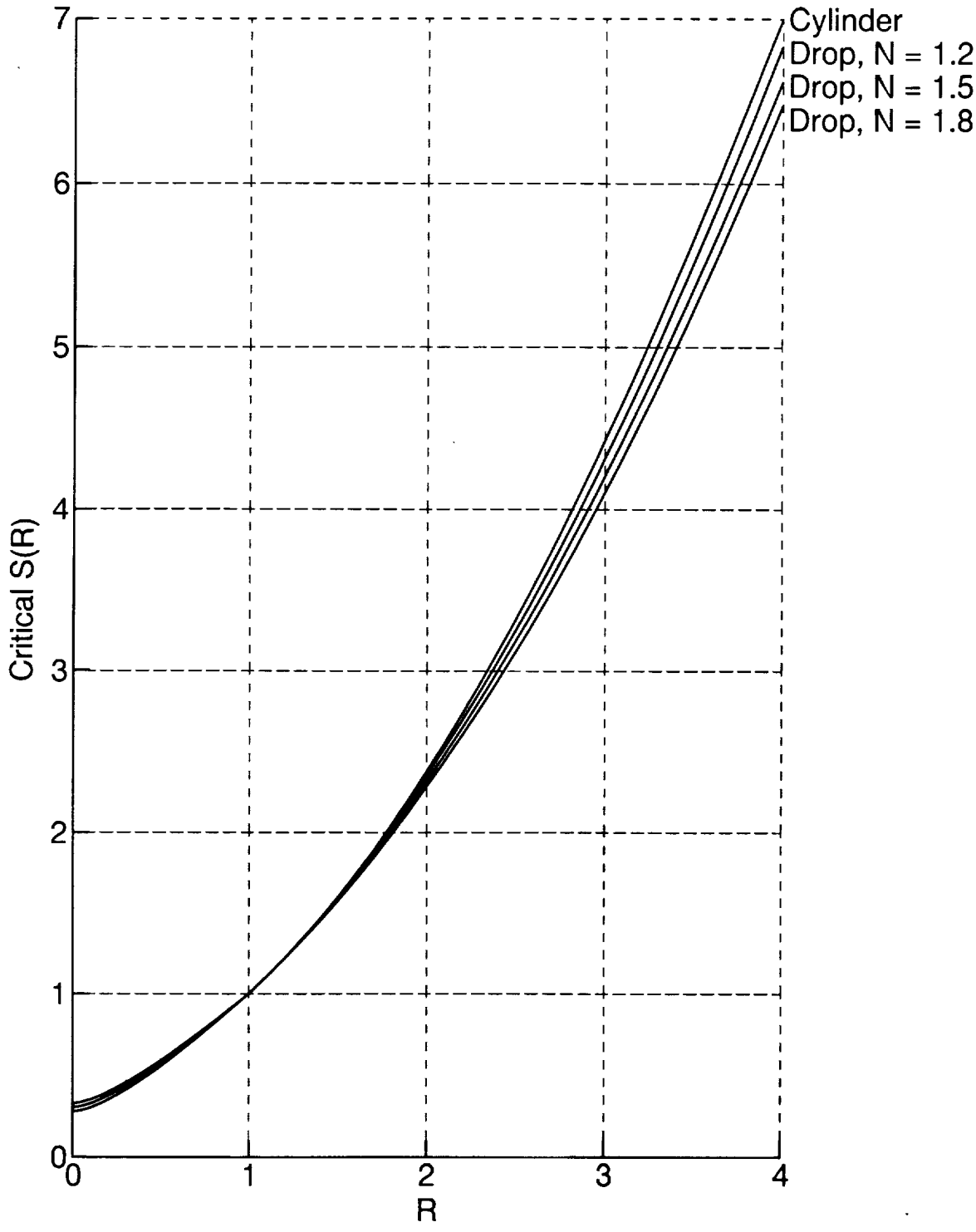

Figure 4. Critical dielectric constant ratio as a function of the conductivity ratio, for drops and cylinders. For drops, N is the function (16) of the viscosity ratio. Below and to the right of the critical value curve, the drop or cylinder elongates in the field direction.

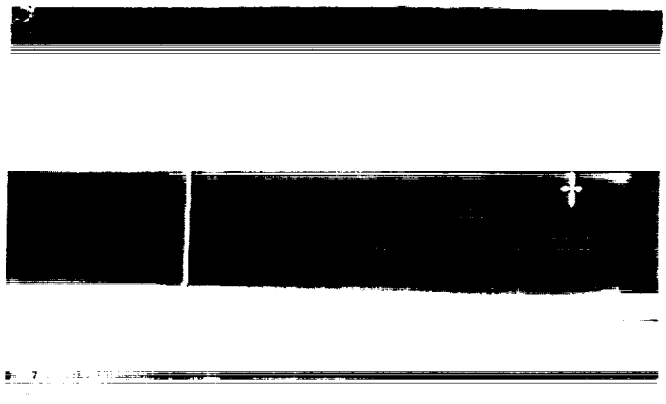

5a. Zero Electric Field

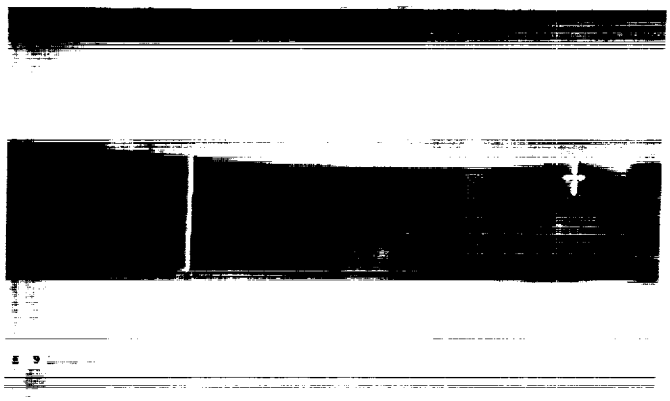

5b. 100 Volts RMS. 100,000 Hz Frequency

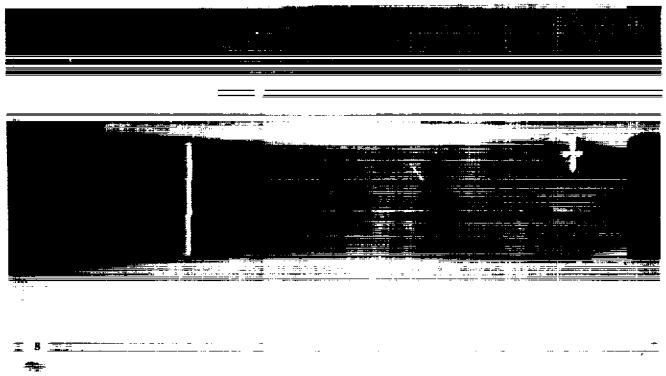

5c. 100 Volts RMS. 50,000 Hz Frequency

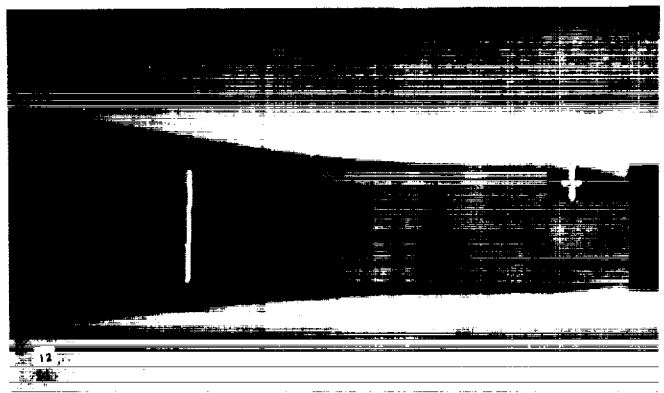

5d. 100 Volts RMS. 10,000 Hz Frequency

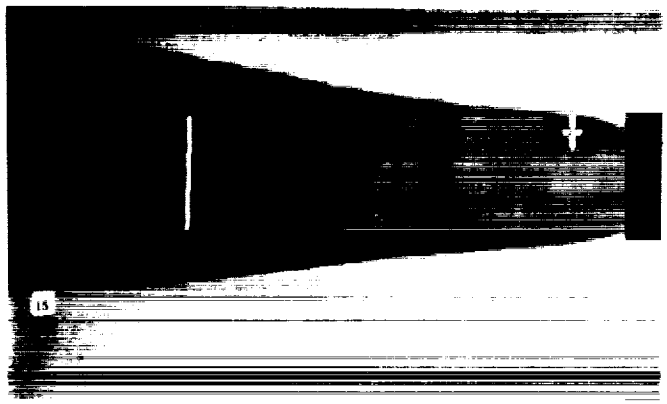

5e. 100 Volts RMS. 5,000 Hz Frequency

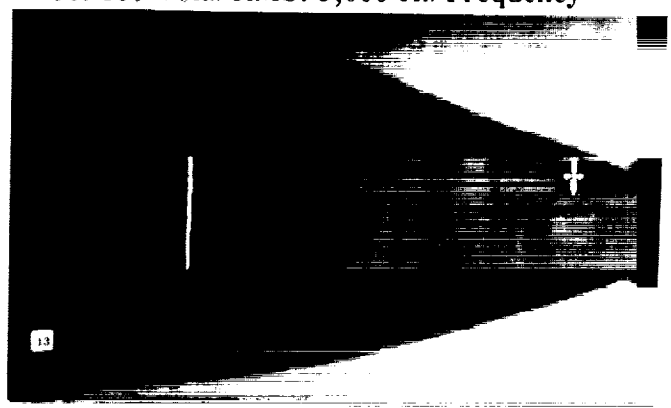

5f. 100 Volts RMS. 1,000 Hz Frequency

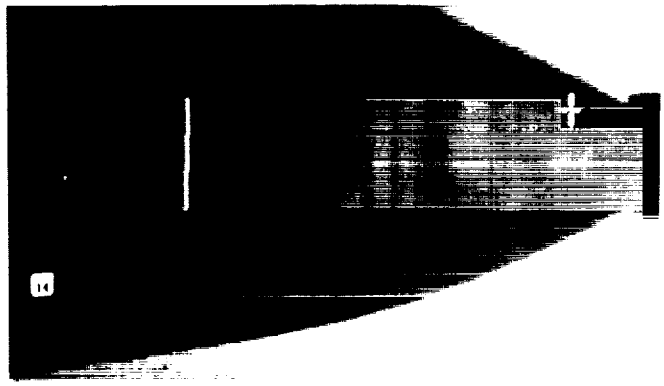

5g. 100 volts RMS. 100 Hz Frequency

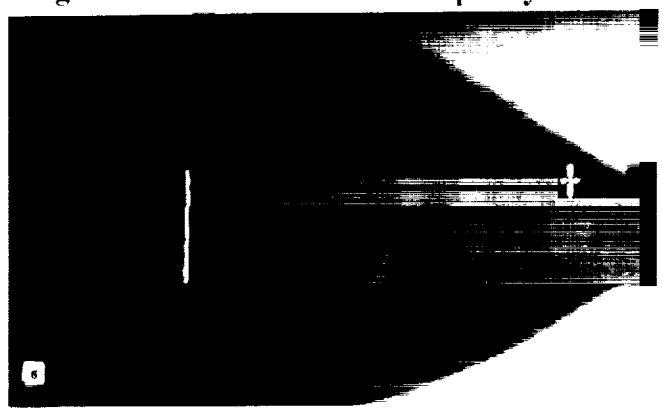

5h. 100 Volts RMS. 28 Hz Frequency

Figure 5 Sample stream distortions viewed parallel to the AC electric fields at varying frequency. 8% PSL